Am J Physiol Cell Physiol 312: C550–C561, 2017.
First published February 8, 2017; doi:10.1152/ajpcell.00219.2015.

RESEARCH ARTICLE | *Molecular Pathways in Cell Signaling*

Identification of a mammalian silicon transporter

Sarah Ratcliffe,[1]* Ravin Jugdaohsingh,[1,2]* Julien Vivancos,[3] Alan Marron,[4] Rupesh Deshmukh,[4] Jian Feng Ma,[5] Namiki Mitani-Ueno,[5] Jack Robertson,[1] John Wills,[6] Mark V. Boekschoten,[7] Michael Müller,[7] Robert C. Mawhinney,[8] Stephen D. Kinrade,[8] Paul Isenring,[9] Richard R. Bélanger,[3] and Jonathan J. Powell[1,2]

[1]*Medical Research Council Elsie Widdowson Laboratory, Cambridge, United Kingdom;* [2]*Department of Veterinary Medicine, University of Cambridge, Cambridge, United Kingdom;* [3]*Département de Phytologie-Faculté des Sciences de l'Agriculture et de l'Alimentation, Centre de Recherche en Horticulture, Université Laval, Quebec City, Quebec, Canada;* [4]*Department of Zoology, University of Cambridge, Cambridge United Kingdom;* [5]*Institute of Plant Science and Resources, Okayama University, Kurashiki, Japan;* [6]*Mechanistic Studies Division, Environmental Health Sciences & Research Bureau, Health Canada, Ottawa, Ontario, Canada;* [7]*Nutrition, Metabolism and Genomics Group, Division of Human Nutrition, Wageningen University, Wageningen, The Netherlands;* [8]*Department of Chemistry, Lakehead University, Thunder Bay, Canada; and* [9]*Nephrology Group L'Hôtel-Dieu de Québec Institution, Department of Medicine, Faculty of Medicine, Université Laval, Quebec City, Quebec, Canada*

Submitted 24 July 2015; accepted in final form 1 February 2017

Ratcliffe S, Jugdaohsingh R, Vivancos J, Marron A, Deshmukh R, Ma JF, Mitani-Ueno N, Robertson J, Wills J, Boekschoten MV, Müller M, Mawhinney RC, Kinrade SD, Isenring P, Bélanger RR, Powell JJ. Identification of a mammalian silicon transporter. *Am J Physiol Cell Physiol* 312: C550–C561, 2017. First published February 8, 2017; doi:10.1152/ajpcell.00219.2015.—Silicon (Si) has long been known to play a major physiological and structural role in certain organisms, including diatoms, sponges, and many higher plants, leading to the recent identification of multiple proteins responsible for Si transport in a range of algal and plant species. In mammals, despite several convincing studies suggesting that silicon is an important factor in bone development and connective tissue health, there is a critical lack of understanding about the biochemical pathways that enable Si homeostasis. Here we report the identification of a mammalian efflux Si transporter, namely Slc34a2 (also termed NaPiIIb), a known sodium-phosphate cotransporter, which was upregulated in rat kidney following chronic dietary Si deprivation. Normal rat renal epithelium demonstrated punctate expression of Slc34a2, and when the protein was heterologously expressed in *Xenopus laevis* oocytes, Si efflux activity (i.e., movement of Si out of cells) was induced and was quantitatively similar to that induced by the known plant Si transporter *Os*Lsi2 in the same expression system. Interestingly, Si efflux appeared saturable over time, but it did not vary as a function of extracellular HPO_4^{2-} or Na^+ concentration, suggesting that Slc34a2 harbors a functionally independent transport site for Si operating in the reverse direction to the site for phosphate. Indeed, in rats with dietary Si depletion-induced upregulation of transporter expression, there was increased urinary phosphate excretion. This is the first evidence of an active Si transport protein in mammals and points towards an important role for Si in vertebrates and explains interactions between dietary phosphate and silicon.

silicon; transport; Slc34a2; *Xenopus laevis* oocytes; rat kidneys

SILICON (Si) is the second most abundant element in the Earth's crust and is ubiquitous in the diet, but the role it plays in mammalian physiology remains unclear. There is substantial evidence for its importance in the normal health and development of bone and connective tissues of vertebrates (6, 25, 43, 45), but a specific physiological and/or metabolic function has not been identified. In particular, proteins responsible for Si transport in mammals remain elusive. Silicon is essential for many algae (e.g., diatoms) to produce their exoskeleton and to complete their cell cycle (5, 21). It is also important in many species of plants, with both structural and physiological roles identified (12, 13, 27).

The first Si transporter to be identified (*Cf*SIT1) was in the diatom species *Cylindrotheca fusiformis* (22), and SITs are now known from a wide range of diatoms (51), choanoflagellates (32), and haptophytes (11). In plants, Si transport occurs through a collaboration of two individual transporter types, one of which is responsible for influx (movement of Si into cell) and the other for efflux (movement of Si out of cell). Influx occurs through an aquaporin channel (e.g., Lsi1, Lsi6) whereas efflux occurs through an energy-dependent active transport process driven by a proton gradient (e.g., Lsi2) (29, 30). Despite the characterization of multiple Si transporters in algae and plants as described, no Si-transporting homologs have been reported in mammals yet (29, 30, 32).

Previously, we reported that Sprague-Dawley rats on a Si-depleted diet massively reduced their urinary Si output to maintain serum and tissue Si levels (24). This was at the expense of phosphorus, which was decreased in serum and bone (24). These findings suggested that the kidney may be actively involved in Si conservation under chronic Si deprivation and that, somehow, phosphate is lost in the process. Here we report on the mammalian phosphate transport protein Slc34a2, which was upregulated in the kidney of the rats deprived of dietary Si. This protein was found to induce Si efflux activity when expressed in *Xenopus* oocytes and to exhibit structural similarity with Lsi2 in many plants. Identification that Slc34a2 can transport Si provides new evidence

* S. Ratcliffe and R. Jugdaohsingh contributed equally to this work.

Address for reprint requests and other correspondence: J. J. Powell, Medical Research Council Elsie Widdowson Laboratory, 120 Fulbourn Road, Cambridge, CB1 9NL, UK (e-mail: jonathan.powell@mrc-ewl.cam.ac.uk and jjp37@cam.ac.uk).

  ISSN 0363-6143.

for a biological role for this element in mammals and establishes another distinct gene family of Si transporters.

MATERIALS AND METHODS

Silicon Depletion Study

Kidneys were obtained from the study of Jugdaohsingh et al. (24) following 6 mo of dietary Si intervention. Three-week-old female Sprague-Dawley rats were maintained for 26 wk on a formulated low-Si feed (~3 μg Si/g feed), with either low-Si drinking water (~15 ng Si/g water; Si deplete group, $n = 20$) or with orthosilicic acid (H_4SiO_4) supplemented in the drinking water (53 μg Si/g water; Si replete group, $n = 10$). A reference group of rats received a normal laboratory maintenance chow diet (B&K Rat and Mouse Standard Diet; B&K Universal) which is naturally high in Si (322 μg Si/g feed) and tap water (5 μg Si/g water); see reference 24 for diet compositions. This third group of rats is referred to as Si-high reference group. Total Si intakes were 0.17 mg Si kg body $wt^{-1}\cdot day^{-1}$ in the Si deplete group, 4.1 mg $Si\cdot kg^{-1}\cdot day^{-1}$ in the Si replete group, and 18.5 mg $Si\cdot kg^{-1}\cdot day^{-1}$ in the Si-high reference group. After 26 wk, rats were euthanized by asphyxiation with carbon dioxide gas as previously described (24). Rats were killed and processed one at a time, with one rat from each group on the same day. Tissues were then harvested, as previously described (24), and stored at −20°C immediately following harvesting and then at −80°C for long-term storage. All groups of rats and their tissues were treated in precisely the same fashion. Spot urine samples were collected from fasted rats (24). Urinary Si and P analysis was by inductively coupled plasma optical emission spectrometry (ICP-OES), as described below, and data were corrected for urinary creatinine (24). As previously described (24), all animal procedures were carried out in accordance with the UK Home Office Animal Scientific Procedures Act 1986 (Scientific Procedures on Living Animals). Use of laboratory animals was approved by King's College London (UK) Animal Ethics Committee and the UK Home Office. For this study, the left kidneys from $n = 10$ Si deplete, $n = 8$ Si replete, and $n = 5$ Si-high reference rats were ground in liquid nitrogen and total RNA was extracted with the Qiagen RNeasy Maxi kit for microarray and quantitative PCR analysis. This part of the study was carried out in 2008.

Gene Array Analysis

Five micrograms total RNA per sample were hybridized to Affymetrix GeneChip Rat Genome 230 2.0 arrays ($n = 4$ Si deplete and $n = 4$ Si replete kidneys). Gene chip robust multiarray analysis (gcRMA) was used to normalize the data including a summarization step based on m-estimator values for the probe sets (58). Modified T-statistics were used to calculate significance of differential gene expression (10, 44) between the Si replete vs. Si deplete groups. Genes were selected as "differentially expressed" when false discovery rate q was < 0.1 (49). [The microarray data set has been submitted to the NCBI Gene Expression Omnibus: accession no: GSE58404.]

Expression Studies

Quantitative real-time PCR was used to investigate the expression of relevant transcripts, including that of an internal control (18S), in the full cohort of rat kidney RNAs ($n = 10$ Si deplete, $n = 8$ Si replete, and $n = 5$ Si-high reference group). Transcripts were amplified with the TaqMan Universal protocol for real-time RT-PCR. The primers were TaqMan Gene Expression Assays consisting of a FAM reporter and TaqMan MGB probes. Differences in gene expression between groups were statistically analyzed by unpaired t-test.

Immunohistochemistry

Kidneys from a normal laboratory maintenance chow fed rat were excised immediately after necropsy and then fixed in 4% PBS-buffered paraformaldehyde. The samples were then cryo-protected via sucrose gradient and snap-frozen in iso-pentane cooled on dry ice. The frozen samples were then embedded in Optimal Cutting Temperature compound (VWR). Tissue sections were subsequently cryo-sectioned at 12 μm thickness, collected on SuperFrost slides (Thermo Scientific), and allowed to air dry overnight at room temperature. Sections were blocked with normal serum in PBS. Samples were then incubated with primary antibody against Slc34a2 (Genetex) or an appropriately matched isotype control. Primary antibody was then detected by incubation with goat anti-rabbit IgG (H+L) Alexa Fluor 488 conjugate (Invitrogen) before counterstaining the nuclei with Hoechst 33342 (Invitrogen) and the cytoskeleton (f-actin) with phalloidin CF633 (Biotium). Imaging was carried out on a Leica SP2 confocal microscope using a 1.2 numerical aperture ×63 water immersion lens. Images were collected using the Leica Application Suite software. Alongside Slc34a2 antibody-stained sections, images of the isotype controls were also collected under identical settings and in "matched" parallel tissue sections. A threshold removing any minor nonspecific signal in the isotype controls was then defined, with this threshold subsequently applied identically across all collected images to robustly identify Slc34a2. Staining for Slc34a2 was distinctly punctate so, as well as presentation in as-collected intensity format, images are also presented in binary format (i.e., all Slc34a2 signal that is brighter than isotype threshold shown at maximum intensity). This "view" was included to facilitate visualization of Slc34a2 locality within the limits of the printed image size.

Urinary P and Si Analyses

Fasting spot urine samples collected from 6-h fasted rats ($n = 8$ Si deplete, $n = 5$ Si replete, and $n = 6$ Si-high reference rats) were digested (in 1:1 mixture of 69% nitric acid and 40% hydrogen peroxide), diluted (1:100), and analyzed for total phosphorus by inductively coupled plasma optical emission spectrometry (ICP-OES; Jobin Yvon 2000-2) at 214.914 nm with sample-based standards. Urinary Si was analyzed by ICP-OES as previously described (24).

Inter-Organism Homology of Si Transporters

Homology search was performed with BLASTp (3) against plant and diatom sequences in the EMBL/GenBank nonredundant protein database using the default settings (http://www.ncbi.nlm.nih.gov/). BLASTp and tBLASTn were also used to identify homologs in a range of fully sequenced vertebrate genomes from the EMBL/GenBank and Ensembl databases, and also to identify homologs in selected phylogenetically relevant groups where complete genomes were not available (see Supplemental Table S1; Supplemental Material for this article is available at the Journal website). An alignment of homologs was generated using MUSCLE (http://www.ebi.ac.uk/Tools/msa/muscle/) under the default settings, producing a final alignment of 38 sequences from 17 species. ProtTest (1) found that the JTT+G+I model provided the best fit to the data under the Akaike Information Criterion. Maximum likelihood analysis was carried out using PhyML (19). Starting trees were generated by BioNJ, with tree searching using the NNI heuristic methods, and topology and branch lengths were optimized in ML calculations. One hundred bootstrap data sets were analyzed using the same model and method as for the PhyML analysis, with bootstrap proportions added as numbers to the nodes of the PhyML tree. The alignment was also used for Bayesian MCMC analysis using Phylobayes 3.3 software (26), under the CAT +G+I model until convergence (maximum discrepancy <0.3, effective size >100), for 15 parallel chains with sampling every 100 cycles and a burn-in equal to one-fifth the total size of the chain. Posterior probabilities were used to express the support for the nodes in the Bayesian phylogeny. The trees generated were viewed using FigTree (version 1.3.1, Andrew Rambaut, Institute of Evolutional Biology, University of Edinburgh 2006–2009).

Calculated Oxoacid Volumes

The structure for each oxoacid/oxoanion was optimized using the PBE0 functional (2, 38, 39) and 6–31++g(d,p) atomic orbital basis set (4, 9, 15, 16, 20, 41, 42). The electron density corresponding to these optimized structures was used to estimate the molecular volume that describes the solvent accessible surface, defined as the volume bounded by a density contour of 0.001 electrons/Bohr^3. An increased density of points was used to ensure a more accurate integration so that the computed molecular volumes are quantitative (37, 56). Since these species are in an aqueous environment, structures were optimized within a solvent field using the integral equation formalism variant of the polarizable continuum model (7, 52, 57) to account implicitly for the effects of an aqueous environment on the solvent accessible surface. The Gaussian09 suite of programs (17) was used in these determinations.

Transport Activity in Xenopus laevis Oocytes

Cloning the gene of interest and oocyte preparation. A cDNA sequence verified *Rattus norvegicus* IMAGE clone pExpress-1/Slc34a2 (Unigene ID: Rn.16933, Entrez Gene: 84395 in DH10BTonA) was purchased from Source BioScience LifeSciences (Cambridge, UK).

For synthesis of capped RNA, the open reading frame (ORF) was amplified by PCR with the following primers: 5′-GAGGATCCATG-GCTCCTTGGCCCGAGTTG-3′ and 5′-GAGGATCCTAGAACAC-TGTAGTGTTGGACA-3′. The fragment containing the ORF was inserted into the *Bgl*II site of a *Xenopus* oocyte expression vector pXßG-ev1 (a pSTP64 T-derived pBluescript type vector into which *Xenopus* β-globin 5′- and 3′-UTR had been inserted) (40). Capped RNA was then synthesized from linearized pXβG-ev1 plasmids by in vitro transcription with mMESSAGE mMACHINE High Yield

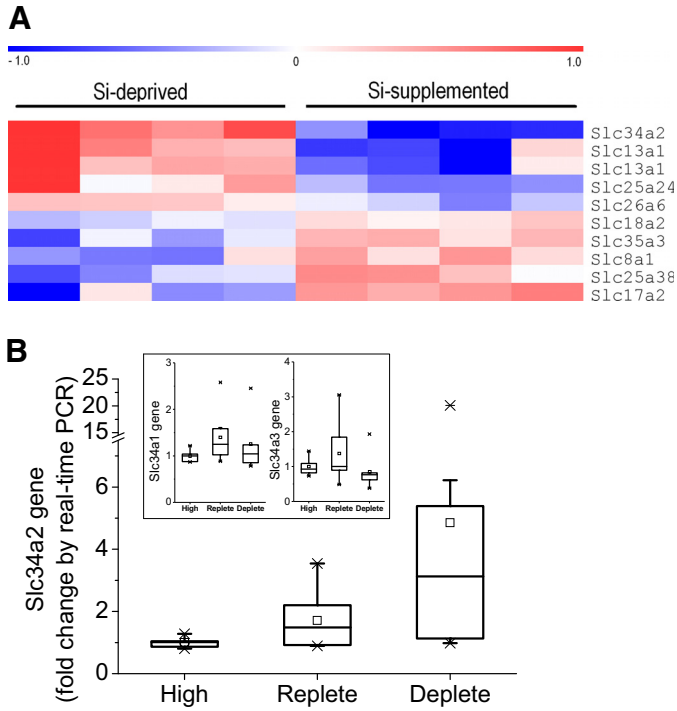

C

```
Slc34a2| MAPWPELENA---HPNPNK---FIEGASG---PQSSIPDKDKG-TSKTNDSGTPVAKIEL
Slc34a1| MMSYSERLGGPAVSPLPVRGRHMVHGAAFAYVPSPQVLHRIPGTTTYAISSLSPVALTEH
Slc34a3| M---PNSLAGDQ-VPNPTLD---AIGLVDWSLRNAGTSGSTPG-----------------
          *            * *        *                *

Slc34a2| LPSYSALVLIEEPPEGNDPWDLPELQDNGIKWSERDSKGKILCIFQGIGKFILLLGFLYL
Slc34a1| SCPYGEVL------ECHDPLPAKLAQEEEQKPEPRLSQ-KLAQVGTKLLKVPLMLGFLYL
Slc34a3| ---------LEEG--GTDPWTFSQLKNTDQLKEVGTAS-KLHQVVSGFLKACGLLGSLYF
                   **                *        *    ** **

Slc34a2| FVCSLDVLSSAFQLVGGKMAGQFFSNNSIMSNPVAGLVIGVLVTVMVQSSSTSSSIIVSM
Slc34a1| FVCSLDVLSSAFQLAGGKVAGDIFKDNAILSNPVAGLVVGILVTVLVQSSSTSTSIIVSM
Slc34a3| FICSLDILSSAFQLLGSKMAGDIFKDNVVLSNPVAGLVIGVVVTVLVQSSSTSSSIVVSM
          * **** ******* * * **  *  *   ******** *  *** ******* ** ***

Slc34a2| VASSLLSVRAAIPIIMGANIGTSITNTIVALMQAGDRNEFRRAFAGATVHDFFNWLSVLV
Slc34a1| VSSGLLEVSSAIPIIMGSNIGTSVTNTIVALMQAGDRTDFRRAFAGATVHDCFNWLSVLV
Slc34a3| VASKSLTVQASVPIIMGVNVGTSITSTLVSMAQSGDRDEFQRAFGGSAVHGIFNWLTVLV
          * *  * *    ***** * *** * * *   * ***  * *** *  **  **** ***

Slc34a2| LLPLEAATHYLEKLTNLVLETFSFQNGEDAPDILKVITDPFTKLIIQLDKKVIQQIAMGD
Slc34a1| LLPLEAATGYLHHVTGLVVASFNIRGGRDAPDLLKVITEPFTKLIIQLDKSVITSIAVGD
Slc34a3| LLPLENATAALERLSELALGAASLQPGGQAPDILKALTRPFTHLIIQLDSSVVTSSITSN
          ***** **  *     *         *  *** **  * *** ******  *

Slc34a2| SEAQNKSLIKIWCKTISNVIEENVTVPSPDNCTSPSYCWTDGIQTWTIQNVTEKENIAKC
Slc34a1| ESLRNHSLIRIWCQP----------ETKEASTSMSRVEAIG----SLANTT----MEKC
Slc34a3| TT--NSSLIKHWCGFRG---------ETPQG--SSEECDLSGSCTERNSSASPGEDRLLC
              * ***  **                    *       *                *

Slc34a2| QHIFVNFSLPDLAVGIILLTVSLLILCGCLIMIVKLLGSVLRGQVATVIKKTLNTDFPFP
Slc34a1| NHIFVDTGLPDLAVGLILLAGSLVVLCTCLILLVKMLNSLLKGQVANVIQKVINTDFPAP
Slc34a3| HHLFAGSELTDLAVGFILLAGSLLVLCVCLVLIVKLLNSVLRGRIAQAVKTVINADFPFP
           * *    * ***** ***  **  ** **   ** * * * *  *       * *** *

Slc34a2| FAWLTGYLAILVGAGMTFIVQSSSVFTSAMTPLIGIGVISIERAYPLTLGSNIGTTTTAI
Slc34a1| FTWVTGYFAMVVGASMTFVVQSSSVFTSAITPLIGLGVISIERAYPLTLGSNIGTTTTAI
Slc34a3| FGWLSGYLAILVGAGLTFLLQSSSVFTAAIVPLMGVGVINLERAYPLFLGSNIGTTTTAL
          * *  ** *  ***  **  ******* *  ** * ***  ****** ***********

Slc34a2| LAALASPGNTLRSSLQIALCHFFFNISGILLWYPIPFTRLPIRLAKGLGNISAKYRWFAV
Slc34a1| LAALASPREKLSSSFQIALCHFFFNISGILLWYPLPCTRLPIRMAKALGKRTAKYRWFAV
Slc34a3| LAALASPADTLLFAVQVALIHFFFNLAGILLWYLVPVLRLPIPLAKRFGDLTAQYRWVAI
          *******   *    * ** *****  ******  *  ****  **  *   * *** *

Slc34a2| FYLIFFFLLTPLTVFGLSLAGWPVLVGVGVPIILLILLVLCLRMLQARCPRILPLKLRDW
Slc34a1| LYLLVCFLLLPSLVFGISMAGWQAMVGVGTPFGALLAFVVLVNVLQSRSPGHLPKWLQTW
Slc34a3| VYLLLTFLLLPLAAFGLSLAGGSVLAAVGGPLVGLVLLIILVNVLQRHRPSWLPRRLQSW
           **   *** *   ** * **       ** *   *          **   *  **  *  *

Slc34a2| NFLPLWMHSLKPWDNIISLATSCFQRRCCCCCRVCCRVCCMVCGCKCCRCSKCCKNLEEE
Slc34a1| DFLPRWMHSLQPLDGLITRATLCYAR-------------------------------PE
Slc34a3| AWLPLWLHSLEPWDRLVT--------GCC-------------------------------
           ** * *** * *

Slc34a2| EKEQDVPVKASGGFDNTAMSKECQDEGKGQVEVLGMKALSNTTVF
Slc34a1| PRSPQLPPRV--------FLEELPPATPSPR--LALPAHHNATRL
Slc34a3  ------PFKA---YSNSHMTSKVAHCYENPQ-VIASQQL------
                 *
```

Fig. 1. Identifying *Rn*Slc34a2 as a candidate for Si transport. *A*: relative expression of solute-like carriers in the kidney of *Rattus norvegicus* from Si deplete ($n = 4$) compared with Si replete ($n = 4$) animals. Data were analyzed by gene array. Red indicates upregulation and blue indicates downregulation of expression; Si replete vs. Si deplete group. Multiple probe sets per gene can be present as was the case for Slc13a1. *B*: quantitative PCR analysis of Slc34a2 and of family members (*inset*) in the kidneys of Si-high reference, Si replete and Si deplete rats. Overall, the relative expression of *Rn*Slc34a2 was inversely related to dietary Si exposure ($P < 0.05$), but there was no relationship with Slc34a1 or Slc34a3 ($P = 0.5$ and 0.4, respectively). Gene expression values are relative to the Si-high reference group. *C*: sequence alignment of the *Rattus norvegicus* Slc34 gene family. Slc34a2 is characterized by a ~30-residue stretch (highlighted in yellow) that is not present in Scl34a1 and Slc34a3. Asterisks (*) below sequence indicate identical amino acids, colons (:) indicate functionally similar amino acids, and dashes (–) indicate gaps in the alignment.

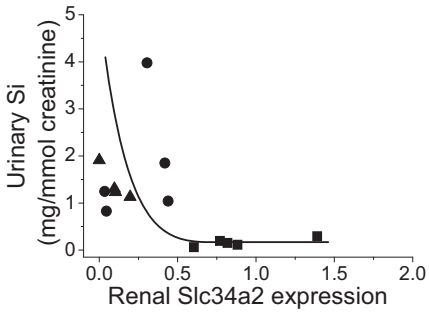

Fig. 2. Correlation between renal *Rn*Slc34a2 expression (by quantitative RT-PCR analysis) and fasting urinary Si excretion. Urinary Si excretion in the rats (■, Si deplete; ●, Si replete) and laboratory chow reference group (▲, Si-high reference) showed an inverse relationship with Slc34a2 expression in the kidneys; $r = 0.47$.

Capped RNA Transcription Kit (Ambion) according to the manufacturer's instructions.

Oocytes were isolated from *Xenopus laevis* frogs purchased from NASCO (Nasco-Fort Atkinson, WI) and from Watanabe Zosyoku (Hyogo Pref, Japan). Procedures for defolliculation, culture condition, and selection were the same as described previously (35). A volume of 50 nl of the in vitro cRNA transcripts (1 ng/nl) was injected into stage V oocytes using a Nanoject II automatic injector (Drummond Scientific). Water-injected oocytes were used as a negative control, *Os*Lsi1-injected oocytes were used as positive controls while testing for influx activity, and *Os*Lsi2-injected oocytes were used as positive controls while testing for efflux activity. Ethical approval was obtained (permit no. 21031043) from the Animal Care Committee of Laval University (Quebec City, QC, Canada).

Influx transport activity. After incubation in a Modified Barth's Saline (MBS) solution (88 mM NaCl, 1 mM KCl, 2.4 mM $NaHCO_3$, 15 mM Tris·HCl at pH 7.6, 0.3 mM $Ca(NO_3)_2$, 0.41 mM $CaCl_2$, 0.82 mM $MgSO_4$, 10 μg/ml sodium penicillin, and 10 μg/ml streptomycin sulfate) at 18°C overnight, the cRNA-injected oocytes were exposed to the MBS solution supplemented with 1 mM H_4GeO_4, 0.1 mM $HAsO_4^{2-}$ or 1 mM HPO_4^{2-} at pH 7.6. Following 30 min incubation at 18°C, the oocytes were washed five times with MBS alone and digested with concentrated (61%) HNO_3. The Ge, As, and P concentrations in the digested solutions were determined by ICP-MS (7700X; Agilent Technologies) with appropriate standards, QCs and sample blanks.

To investigate the Si influx and its dependence on extracellular $[Na^+]$ or $[HPO_4^{2-}]$, oocytes were incubated for three days at 18°C in MBS5 (84 mM Na^+ and 2 mM HPO_4^{2-}) supplemented with 100 μM each of penicillin and streptomycin. Then a set of 10 oocytes for each condition was exposed to MBS2 (1.7 mM H_4SiO_4, 10 mM Na^+, and 0.5 mM $HPHPO_4^{2-}$) or MBS3 (1.7 mM H_4SiO_4, 84 mM Na^+, and 2 mM HPO_4^{2-}) solution for 2 h. After exposure, oocytes were rinsed in a solution containing 0.32 M sucrose and 5 mM HEPES (pH 7.4) and then digested in 25 μl concentrated nitric acid, dried at 82°C for 2 h, reconstituted in plasma grade water (100 μl) and 10 μl analyzed by atomic absorption spectroscopy (see below).

Efflux transport activity. To investigate the efflux transport activity for H_4GeO_4 by *Rn*Slc34a2, 50 nl 1 mM H_4GeO_4 in MBS were directly injected into *Rn*Slc34a2-transfected oocytes. The oocytes were then washed five times with MBS and transferred to 200 μl of fresh MBS at 18°C. H_4GeO_4 was allowed to efflux into the incubation medium.

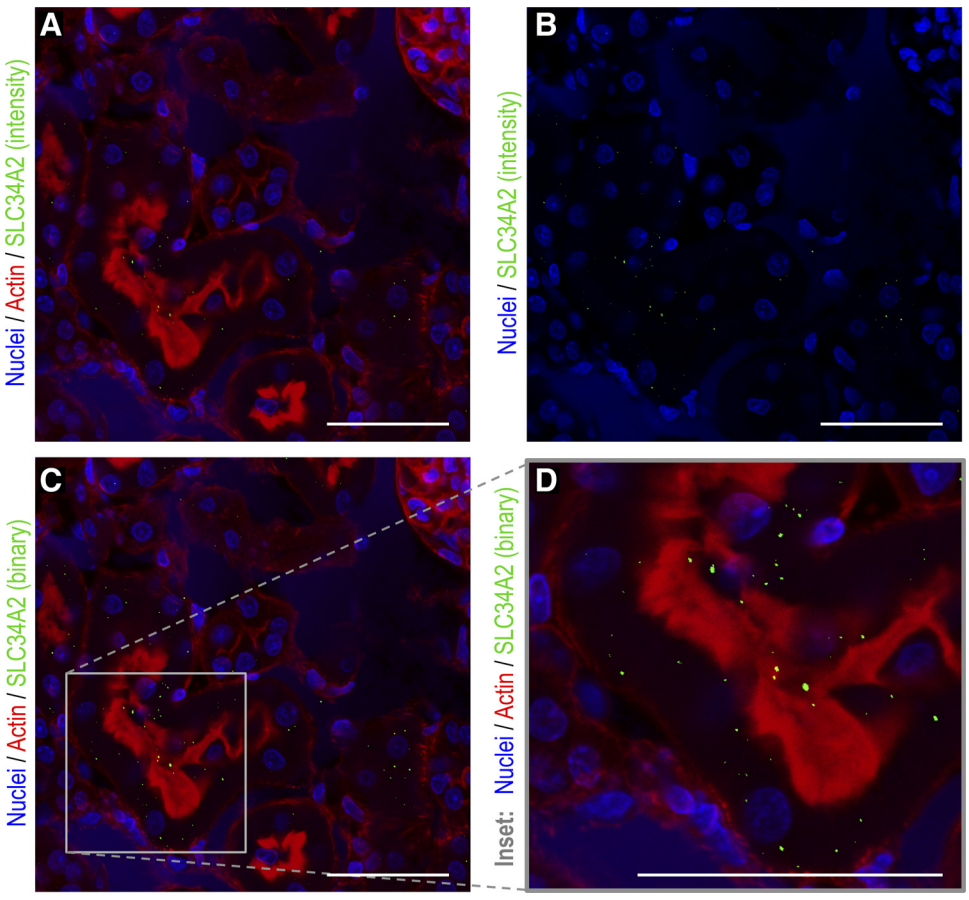

Fig. 3. Immunohistochemistry analysis of Slc34a2 in freshly harvested rat kidney cortex. Sections of freshly harvested kidneys from a healthy wild-type rat were analyzed by immunohistochemistry with anti-Slc34a2 (*green*) antibody (this figure) or the appropriate isotype control (data not shown). Cell nuclei were counterstained (*blue*) with Hoescht 33342 and cell cytoskeleton (f-actin, *red*) with phalloidin CF633. Antibody-stained sections and isotype controls were collected under identical settings, as stated in MATERIALS AND METHODS. A threshold removing all Slc34a2 attributable signal was defined on the isotype controls and uniformly applied to all images (i.e., antibody-stained images). Staining for Slc34a2 within the tubular epithelial cells was distinctly punctate so, as well as the signal above the isotype control being presented in an as-collected "intensity" format (i.e., the more secondary antibody that is bound, the brighter the signal) (*A* and *B*), it is also displayed as a binary format (i.e., all signal that is brighter than isotype threshold is given the maximum intensity value) as this aids visualization (*C* and *D*). All images are of the kidney cortex and scale bars are 50 μm. *B*: as-collected "intensity" format without actin staining. *D*: a high-power image (×63 magnification) of the area within the quadrant in image (*C*).

A

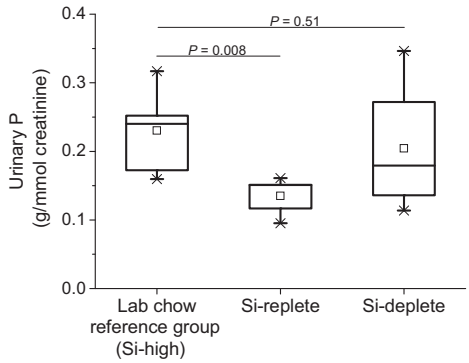

B

	Lab chow reference group (Si-high)	Si -replete	Si-deplete
Renal Slc34a2 (relative expression)*	0.336 ± 0.062	0.574 ± 0.308	1.63 ± 1.90
Si (μg/g feed)	322 ± 47	3.2 ± 0.6	3.2 ± 0.6
Si (μg/g drinking water)	5.04 ± 1.12	53.2 ± 0.6	0.015 ± 0.010
P (g/kg feed)	7.00	2.28	2.28

*Summarised from Figure 1b

Fig. 4. Fasting urinary phosphorus excretion. Urinary P excretion was measured in the laboratory chow reference group (Si-high reference; $n = 6$), Si replete ($n = 5$), and Si deplete ($n = 8$) rats by ICP-OES and corrected for creatinine concentration (*A*). The higher P excretion in the laboratory chow reference group is due to the higher P content of the diet (see *B*). However, the difference in urinary P excretion between the Si replete and Si deplete rats cannot be explained by a difference in dietary P content, but rather due to the upregulation of Slc34a2 in the latter group mediated by Si deficiency in the diet and drinking water (*B*).

After 30 min and 2 h, the incubation medium was carefully sampled, and at the end of the experiment, the oocytes were digested with concentrated HNO_3 and the samples were analyzed for Ge by ICP-MS (7700X) with appropriate standards, QCs, and sample blanks.

To investigate the efflux transport activity for Si by *Rn*Slc34a2, oocytes were injected with 25 nl of 500 ng/nl cRNA of *RnSlc34a2* or *OsLsi2* or an equal volume of H_2O as a negative control. Pools of 10 oocytes were then loaded with Si by incubation for three days at 4°C in MBS1 or MBS2, both containing 2 mM Si but different concentrations of Na^+ and HPO_4^{2-} (Supplemental Table S2). These oocytes were then exposed to fresh MBS without added Si but with different concentrations of Na^+ and HPO_4^{2-} (MBS, MBS3, MBS4, or MBS5 solution; Supplemental Table S2) for 0, 1, or 2 h. After exposure, oocytes were rinsed in a solution containing 0.32 M sucrose and 5 mM HEPES (pH 7.4), digested with concentrated HNO_3 (25 μl for each pool of 10 oocytes) and dried at 82°C for 2 h. Plasma-grade water (100 μl) was then added, and samples were incubated for 1 h at room temperature. Samples were vortexed and then centrifuged for 5 min at 13,000 *g*. Ten microliters of samples were then analyzed by Zeeman atomic absorption spectrometer (Varian AA240Z; http://www.varian.com) equipped with a GTA120 Zeeman graphite tube atomizer, to determine the intracellular Si concentration. Silicon levels in the samples and sample blanks were quantified using appropriate standards prepared using 1,000 ppm ammonium hexafluorosilicate solution (Fisher Scientific, http://www.fishersci.com). Data were analyzed with SpectrA software (Varian).

Statistical Analysis

Results are reported as means ± SD unless otherwise stated. Linear relationships between dietary Si exposure and the relative renal expression of Slc34 genes were assessed at a significance of $P \leq 0.05$. Thereafter, individual differences were assessed by Independent (unpaired) Samples 2-Tailed T-test. Where there were multiple group comparisons a Bonferroni correction was applied to the *P* value (i.e., P/n), and significance was taken as $P \leq 0.05/n$. All statistical analysis was conducted in GraphPad Prism (version 6.0b) or IBM SPSS software (version 21; IBM).

RESULTS AND DISCUSSION

Identifying RnSlc34a2 As a Candidate for Si Transport

Data from our study of Si deficiency in rats strongly suggested active urinary conservation of Si during dietary Si depletion (24). The present investigation utilized kidneys harvested during this study to investigate Si regulatory genes. Gene arrays (Affymetrix GeneChip Rat Genome 230 2.0 arrays containing over 16,000 Entrez IDs and 11 probes per gene) were performed on RNA extracted from the kidney tissues of Si deplete and Si replete rats ($n = 4$ for each group) and the data were interrogated for differential regulation of potential transporters (Fig. 1*A*). The gene array findings[1] were confirmed by real-time RT-PCR analysis, and this technique was also subsequently used to investigate a larger cohort of samples from the Si deplete ($n = 10$), Si replete ($n = 8$), and a reference group ($n = 5$) that were rats kept on a normal laboratory chow diet that is naturally high in Si (referred to as Si-high reference group). Slc34a2 (type II sodium-phosphate cotransporter), commonly referred to as NaPi-IIb, was expressed especially highly in the kidneys of rats on the Si deplete diet (2.8- and 4.8-fold higher than for kidneys from rats on the Si replete and Si-high reference diets, respectively; Fig. 1*B*). mRNA expression of other Slc34 family members, namely Slc34a1 and Slc34a3, were unchanged with dietary Si intervention (*inset*, Fig. 1*B*).

Correlation between Slc34a2 expression and urinary Si concentration showed an inverse exponential relationship between fasting urinary Si level and the relative expression of Slc34a2 (Fig. 2), implying that Slc34a2 is involved in the reabsorption of H_4SiO_4 from the pre-urine under dietary Si

[1] Gene array data have been submitted to the Gene Expression Omnibus repository and assigned the reference GSE58404.

Table 1. *Oxoacid and oxoanion volumes*

Oxoacid/Oxoanion	Gas Phase V_M, cm^3/mol	Implicit Aqueous Solvent V_M, cm^3/mol
HCO_3^-	41.9	39.1
H_3BO_3	43.4	43.6
$H_4BO_4^-$	52.5	55.8
H_4SiO_4	63.2	56.5
H_4GeO_4	61.3	57.8
HPO_4^{2-}	62.0	59.2
$HAsO_4^{2-}$	65.0	63.1

PBE0/6–31++g(d,p) calculated solvent accessible surface molar volumes (V_M) for various main group oxoacids and oxoanions at physiological pH, showing the similarities between H_4SiO_4, H_4GeO_4 (two oxoacids that are effluxed by Slc34a2), HPO_4^{2-}, and $HAsO_4^{2-}$ (oxoanions that are influxed by Slc34a2).

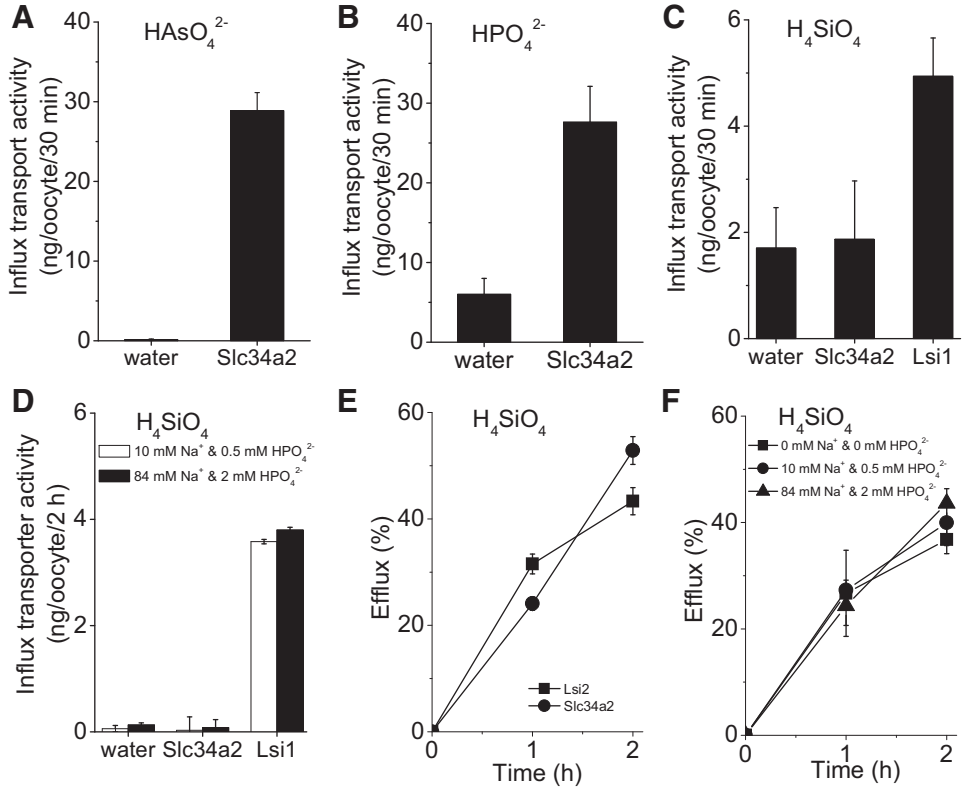

Fig. 5. Transport activity in *Rn*Slc34a2-expressing oocytes. *A–C*: influx transport activity of *Rattus norvegicus* Slc34a2 for arsenate, $HAsO_4^{2-}$ ($P = 0.0001$) (*A*), phosphate, HPO_4^{2-} ($P = 0.0008$) (*B*), and silicic acid, H_4SiO_4 ($P = 0.66$) (*C*) . Rice transporter Lsi1 was used as a positive control for H_4SiO_4 influx ($P < 0.0001$). *D*: the concentrations of sodium and phosphate in the medium did not influence H_4SiO_4 influx by *Rn*Slc34a2-expressing oocytes, nor that by *Os*Lsi1-expressing oocytes ($P < 0.0001$ in both instances). Water-injected oocytes were used as a negative control. *E*: in H_4SiO_4 efflux studies, rice transporter Lsi2 was used as a positive control. Data were corrected against water-injected control oocytes. *F*: changes in sodium and phosphate concentration did not affect H_4SiO_4 efflux by Slc34a2 expressing oocytes. Data are shown as means ± SE ($n = 15$).

deprivation. No such relationship was observed for Slc34a1 and Slc34a3, or other candidate transporters identified in the gene arrays (Fig. 1*A*).

Only a few reports have demonstrated the renal expression of Slc34a2. The original paper characterizing the transporter demonstrated its presence in murine kidney at the mRNA level (23). Suyama et al. (50) confirmed this more recently by in situ hybridization as well as protein expression and localization by antibody staining. The kidney samples from our study were not adequately collected for immunohistochemical analysis, but were for RNA analysis. Thus we confirmed with appropriately collected kidneys from a control rat that, as previously published (50), Slc34a2 protein is expressed by the tubular epithelial cells of the kidney cortex (Fig. 3). Here, as previously reported (50), Slc34a2 showed distinct punctate staining: some of which was basolateral within the cell and some of which was apical/cytosolic (Fig. 3). Whether silicate deficiency dictates only the level of expression of Slc34a2 (Fig. 1) or, also its precise location in the cell, as excess dietary phosphate does (50), should be investigated in future work.

Finally, to translate these observations (i.e., that Slc34a2 has some basolateral expression in kidney cells and is upregulated in Si deplete diets) we measured urinary P excretion in the three groups. The Si-high reference group diet was higher in P than the Si replete group diet, being 7.0 vs. 2.3 mg/g, respectively, and so, as expected, urinary P excretion was significantly reduced in the latter [by 89 mg/mmol creatinine for the medians; $P = 0.008$; $n = 6$ and 5, respectively (Fig. 4)]. However, the Si deplete group (with the same dietary P level as the Si replete group) showed no difference in urinary P levels compared with the reference group (Fig. 4), showing that in this group, phosphate was being (relatively) wasted as a consequence of Si being conserved.

RnSlc34a2 Transport Activity

The ubiquitous nature of Si makes transport studies of soluble silicic acid (H_4SiO_4) challenging. It is well known that related oxoacids may ride the same transport systems (22, 29, 36, 54) owing to similarities in their structure and solvated molecular volume (Table 1). Germanic acid (H_4GeO_4), the

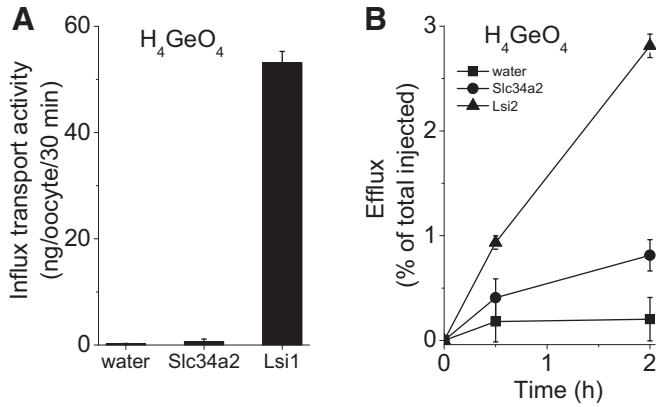

Fig. 6. Germanium transport activity in *Rn*Slc34a2-expressing oocytes. Transport activity for H_4GeO_4 showing a lack of influx ($P = 0.14$) (*A*) but significant efflux (*B*) following a 2 h incubation ($P = 0.004$). Efflux was not significant at 30 min ($P = 0.14$) for Slc34a2-expressing oocytes. The rice Si transporters Lsi1 and Lsi2 were used as positive controls for influx and efflux activity, respectively ($P < 0.0001$ in both cases compared with negative control, water-injected oocytes).

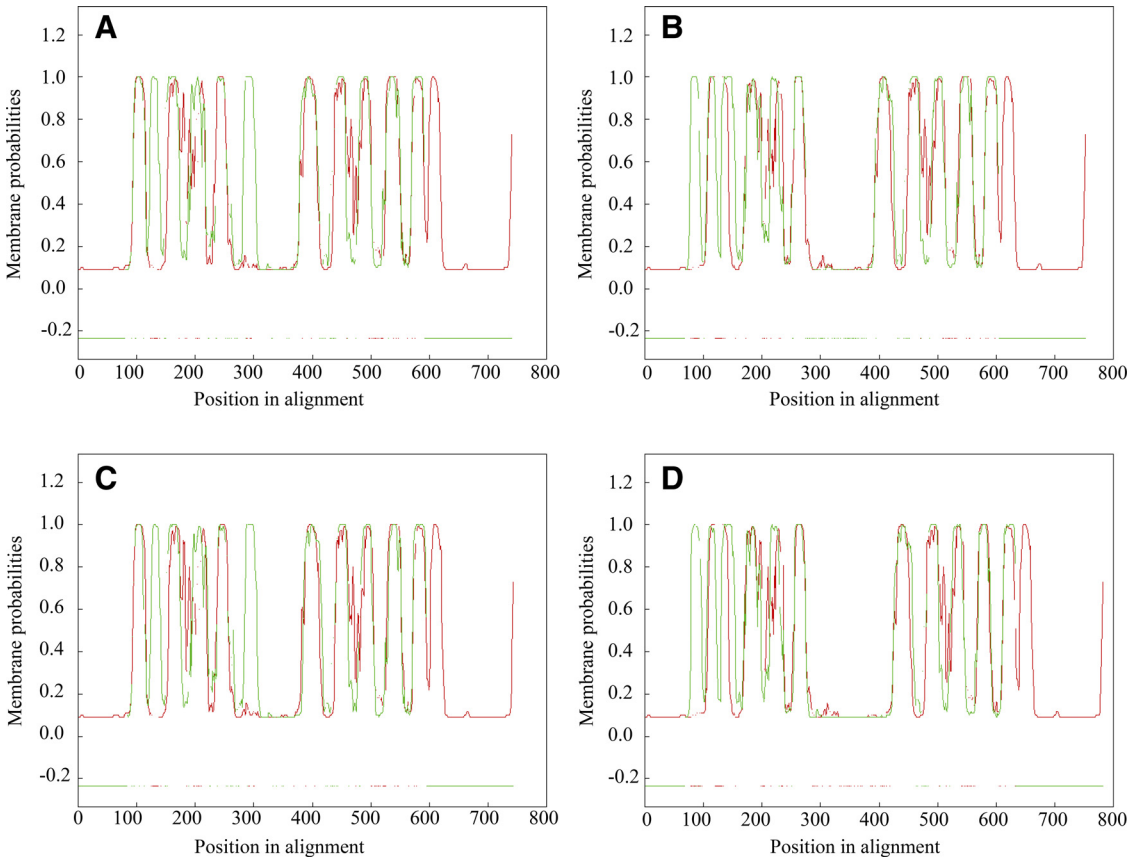

Fig. 7. Pairwise alignment of the transmembrane domains of Si efflux transporters. Pairwise alignment of the transmembrane domains predicted in *Rn*Slc34a2 rat protein (red) with the four Si efflux transporters in plants (green). Transmembrane domains were predicted by OCTOPUS (56), and subsequent alignment was performed by AlignMe tool (51). *A*: *Os*Lsi2 (rice); *B*: *Zm*Lsi2 (maize); *C*: *Hv*Lsi2 (barley); *D*: *Cm*Lsi2–1 (pumpkin).

closest structural analog of silicic acid, is therefore often employed as a proxy for Si transport, thereby avoiding all background and contamination issues with Si and facilitating analysis (22, 29). Recently, however, graphite furnace atomic absorption spectrometry (GFAAS) was shown to be effective for directly measuring Si influx/efflux in *Xenopus laevis* oocytes transfected with Si-transporting aquaporins from plants (8, 18). Hence, both methods of characterizing Si transport— indirect and direct—were used in the present investigation.

The Slc34a2 coding sequence was inserted into a *Xenopus laevis* expression vector, and cRNA synthesized from this construct was injected into oocytes. Initial expression and plasma membrane localization were verified using an eGFP-tagged Slc34a2 construct. Slc34a2 is recognized as a sodium phosphate importer, especially in the brush border of small intestine membrane cells (14, 31, 36, 55), and arsenate also rides this transport system (36, 54). Therefore, both of these oxoacids were utilized as easily measured probes to confirm Slc34a2 influx activity (Fig. 5, *A* and *B*). The rice Si importer *Os*Lsi1 was used as a positive control and was found to promote both H_4SiO_4 (Fig. 5*C*) and H_4GeO_4 (Fig. 6*A*) influx. By contrast, no influx of either H_4SiO_4 or H_4GeO_4 by Slc34a2-expressing oocytes was observed (Figs. 5*C* and 6*A*). On the

Table 2. *Predicted transmembrane domains of Slc34a2*

Helix No.	NH_2 Terminus	Transmembrane Region	COOH Terminus	Helix Type	Length, a.a.
1	95	FQGIGKFILLLGFLYLFVCSLDV	117	1°	23
2	137	NSIMSNPVAGLVIGVLVTVMVQS	159	2°	23
3	166	IIVSMVASSLLSVRAAIPIIMGA	188	2°	23
4	374	LILCGCLIMIVKLLGSVLRGQVA	396	1°	23
5	422	VGAGMTFIVQSSSVFTSAMTPLI	444	1°	23
6	459	LGSNIGTTTTAILAALASPGNTL	481	2°	23
7	527	WFAVFYLIFFFLLTPLTVFGLSL	549	1°	23
8	555	LVGVGVPIILLILLVLCLRMLQA	577	1°	23
9	618	CCCCCRVCCRVCCMVCGCKCCRC	640	2°	23

The transmembrane domains were predicted using SOSUI software. The sequence highlighted in yellow through multiple sequence alignment of the three *Rattus norvegicus* Slc34 family members (Fig. 1*C*) is present in the ninth transmembrane helix of Slc34a2 (shown in bold). The COOH-terminal and NH_2-terminal amino acids for each transmembrane domain are indicated, as is the type of α-helical structure (i.e., primary or secondary helices, denoted as 1° and 2°, respectively).

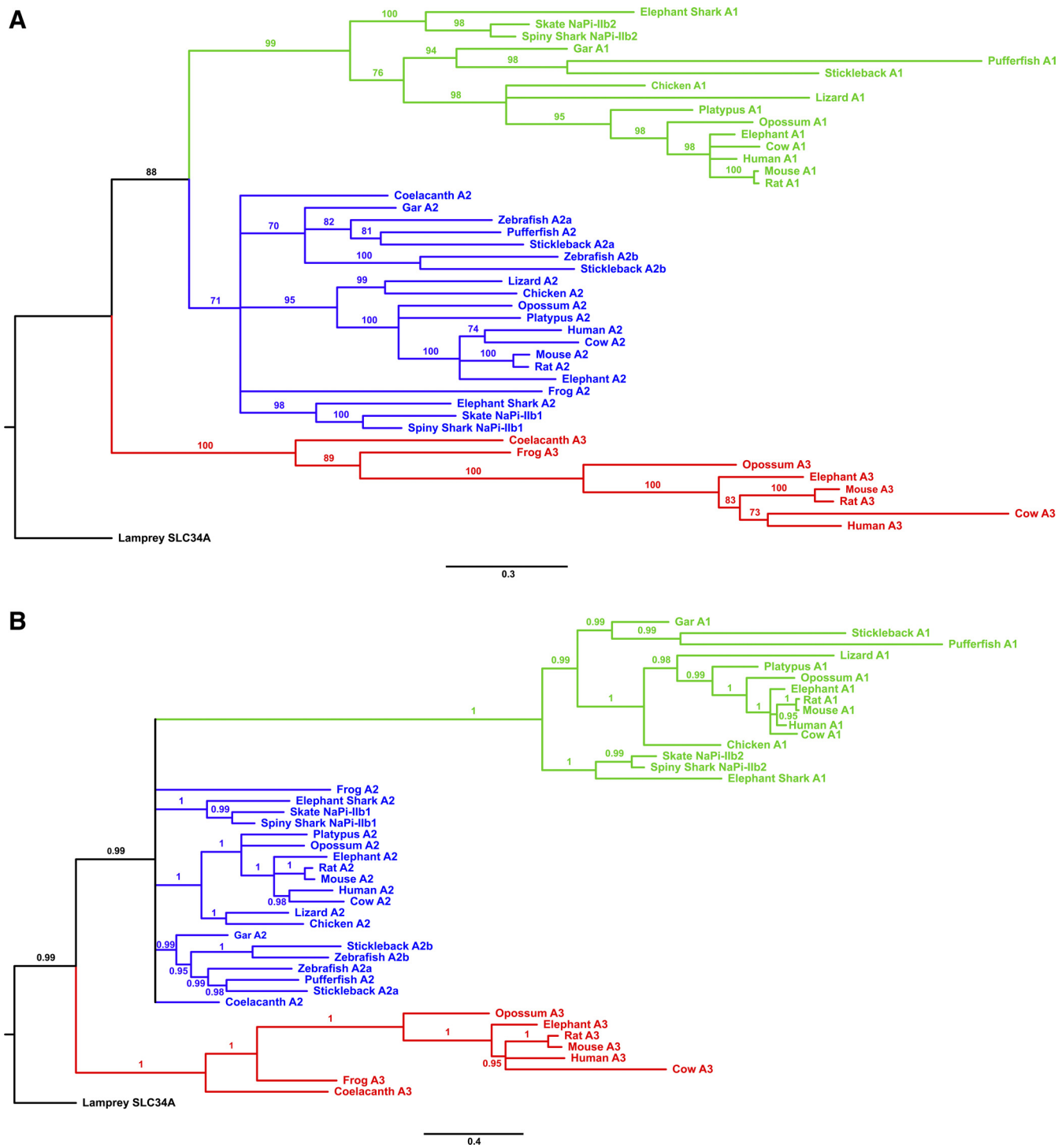

Fig. 8. Phylogeny of Slc34a gene family member in vertebrates. *A*: the tree was produced using PhyML maximum likelihood analysis with the JTT+G+I model from an alignment of 880 positions. Numbers at nodes are a percentage of 100 bootstrap replicates, with nodes having <70% bootstrap support being collapsed. *B*: the tree was produced using Phylobayes Bayesian MCMC analysis under the CAT +G+I model (15 parallel chains with sampling every 100 cycles, burn-in one-fifth the total size of the chain) from an alignment of 880 positions. Numbers at nodes indicate posterior probabilities, with nodes having <0.95 support being collapsed. The scale bar indicates the average number of amino acid substitutions per site. The Slc34a1 clade is in green, the Slc34a2 clade is in blue, and the Slc34a3 clade is in red. The trees are rooted using the single Slc34a homolog identified from the lamprey genome. The Slc34a gene phylogeny largely agrees with the species phylogeny for vertebrates (33), with incongruent branches (e.g., the basal branches of the a2 clade) only having low statistical support. The maximum likelihood phylogenetic analyses resolve that the Slc34a clade evolved from a single ancestor in jawless vertebrates, and likely involved two main duplication events, initially producing the a3 and a1+2 clades, with a further divergence of the a1 and a2 clades. A teleost-specific duplication event resulted in the evolution of Slc34a2a and Slc34a2b, as found in stickleback and zebrafish. The Bayesian analysis had poor phylogenetic resolution at the base of the a2 clade, but still resolves the a1 and a3 groups as distinct monophyletic clades, and is not incongruous with the maximum likelihood analysis results. For full details of the species and sequences used see Supplemental Table S1.

other hand, efflux of both H_4SiO_4 and H_4GeO_4 was detected for oocytes expressing Slc34a2 (Figs. 5*E* and 6*B*, respectively) as well as those expressing rice Si exporter *Os*Lsi2, which was employed as a positive efflux control. Of note, the magnitude of fractional H_4SiO_4 efflux after 2 h was quantitatively similar between Slc34a2 and *Os*Lsi2.

Given that inward phosphate (HPO_4^{2-}) transport by Slc34a2 is coupled to the inward transport of three sodium ions [i.e., it is electrogenic (14, 55)], we investigated how varying the concentrations of Na^+ and HPO_4^{2-} in the external medium might influence Si influx and efflux in Slc34a2-expressing oocytes. No significant effects were observed at the broad concentrations investigated (Figs. 5, *D* and *F*). These findings suggest that Si is not translocated across the membrane through the Na^+ or HPO_4^{2-} transport site, but through an independent transport site that is potentially involved in Si efflux primarily. In keeping with this possibility is the presence of multiple, often independent binding sites in a number of ABCD family members (47). Alternatively, Slc34a2 could cooperate with accessory proteins to promote Si efflux. In this regard, the Na^+-K^+-ATPase γ-subunit FXYD2 appears to play a role in Mg^{2+} transport, while the α- and β-subunits alone do not exhibit such transport capabilities (46).

Homology Between Slc34a2 and Si Transporters

Comparative sequence analysis of Slc34a2 indicated no significant homology with known plant or algal Si transporters. However, marked similarities were revealed upon pairwise alignment of the transmembrane domains of Slc34a2 and the plant Si efflux transporter Lsi2 (Fig. 7), thereby suggesting a conserved structure among Si efflux proteins.

Phylogenetic Analysis of the Slc34 Family

Sequence alignment within the rat Slc34 gene family led to the identification of a ~30-residue stretch that is only present in Slc34a2. Given that Slc34a1 and Slc34a3 were not upregulated under Si deprivation, this finding points towards the possibility that the ~30-residue stretch conveys Si transport activity to Slc34a2 (Fig. 1*C* and Table 2).

Phylogenetic analysis of the Slc34a genes from a range of vertebrates (Supplemental Table S1 and Fig. 8) showed that the family underwent an expansion relatively early in vertebrate evolution, resulting in three distinct main groups (a1, a2, and a3) among the modern jawed vertebrates. At least one member of the a2-group was found in all of the jawed vertebrate genomes searched. In contrast, losses of the a1- and a3-group

```
Pufferfish Slc34a1      NWDFFPIWMTSLQPIDDLITRMS-------------------------RVCRQNRGWWRI--HRNRSTTPLERGTVHTVTN
Stickleback Slc34a1     SWDFLPKWMRSLKPLDRLITKATA------CGCS-------------GHQDARGEDGGDGRMSTKEIVRESAQKME----QL
Lizard Slc34a1          SWDFLPFWLRSLQPMDGLITRTMR------CCTV-------CCSYSREKHSATSPQMKAKLGLCNPSLSFLGELSLPPKPSS
Gar Slc34a1             SWDFLPGWMHSLKPMDAFITNATL------CCTV---------------HCSTKNSDVQGQPVFSDSFAEKKAKMA------
Elephant Shark Slc34a1  NWDFLPIWMHSLKPMDRVITNVTL------YCT----------------NHCRCSEKTDLKEVNCQQERSPQLKEK----AV
Chicken Slc34a1         SWDFLPAWMHSLQPLDSLITRATL------CCT----------------DRCRSPEGWD----EREAAARDKARLGLDNPVL
Opossum Slc34a1         TWDFLPYWMHSLKPLDRLITRATL------CCTH---------------PEPRSPPLPTRVYLEELPTATPSPRLGVLPPDT
Platypus Slc34a1        TWEFLPRWMRSLKPLDGLITRATL------CCAH---------------ADPAKSPRLPARATYDNPGARVYLQEL----PR
Cow Slc34a1             TWDFLPLWMHSLKPLDRLITRATL------CCAR---------------AEPRSPPLPARVFLEELPPATPSPHLA------
Mouse Slc34a1           TWDFLPRWMHSLQPLDGLITRATL------CYAR---------------PEPRSPQLPPRVFLEELPPATPSPRLA------
Rat Slc34a1             TWDFLPRWMHSLQPLDGLITRATL------CYAR---------------PEPRSPQLPPRVFLEELPPATPSPRLA------
Elephant Slc34a1        TWDFLPQWMHSLKPLDHFITRATL------CCAR---------------PEPRSPPMPRRVFLEELPPATPSPHLA------
Human Slc34a1           TWDFLPRWMHSLKPLDHLITRATL------CCAR---------------PEPRSPPLPPRVFLEELPPATPSPRLA------
Frog Slc34a2            NWDFLPKWMHSLKPWDSCMGGASL-LCRHFCCCC-------CGKMCKPCKCCKCCHDK-----EDEEYSIEPKPQA----LE
Platypus Slc34a2        NWDFLPKWMHSLKPWDSVVSGLTG-SFRKCCCCC-----RICCMLCGCPPCCRCSKCCRDSGTEDEEPAKDIPVKG----GE
Opossum Slc34a2         NWHFLPLWMRSLQPWDGIVSLLTGNCCQLPCCWCCRACCRVCCLLCGCPRCCRCSKCCDLL--EEEENVKEIPIKV----PE
Cow Slc34a2             SWDFLPFWMRSLEPWDKLITSLTS-CFQMRCCCCCRVCCRLCCGLCGCSKCCRCTKCS-----EDLEEGKDEPVKS----PE
Elephant Slc34a2        NWNFLPLWMHSLKPWDHLISLLTS-CCQ-RCCCC---CCHLCCVLCGCPKCCRCNKYLEDL-EEGQEYSKDTPIKT----PN
Human Slc34a2           NWNFLPLWMRSLKPWDAVVSKFTG-CFQMRCCCCCRVCCRACCLLCGCPKCCRCSKCCEDL--EEAQEGQDVPVKA----PE
Mouse Slc34a2           DWNFLPLWMHSLKPWDNVISLATT-CFQRRCCCCCRVCCRVCCMVCGC-KCCRCSKCCRDQGEEEEEKEQDIPVKA----SG
Rat Slc34a2             DWNFLPLWMHSLKPWDNIISLATS-CFQRRCCCCCRVCCRVCCMVCGC-KCCRCSKCCKNL--EEEEKEQDVPVKA----SG
Lamprey SLC34a          TWNFLPDWMHSMKPLDRVISAVCG-----RCCKC-------C-------KCVSKSGK------NKQVEVVSIPDST------
Zebrafish Slc34a2b      SWDFLPLWAHSLDPWDRVVTVIAA-----RCCCC-------C-------KCCNSNEEDEKAKLENLANGIEINDNT------
Stickleback Slc34a2b    SWDFLPLWAHSLSPWDKVVGVFTA-----KCCCC-------C-------KCCQFADD------DKETGETESLENNSKSHTE
Pufferfish Slc34a2a     SWDFLPRPLHSLAPWDAVVTSMLG-FCGNRCCCC-------C-------KCSNCCQR------NDEEAVR---KGS----LE
Stickleback Slc34a2a    SWDFLPRPMRSLAPWDAVVTSAFG-FCGKHCCCC-------C-------KCCKCCRK------KEDEKVMNQGRKS----LE
Zebrafish Slc34a2a      SWEFLPKPLHSLKPWDRVVTAGMS-FCRTRCCCC-------C-------KCCR----------NEEKNHMENNDRS----LE
Gar Slc34a2             TWEFLPKWMHSLKPWDRVITSMLS-FCRTRCCCC-------C-------KCCNKIS-------SEEDGTGKEKRGS----LE
Coelacanth Slc34a2      TWDFLPLWMHSLHPWDKVITSMMG-YCGSHCCKC-------C-------KCCR-MVH------AEDAGVKEKQVES----LH
Elephant Shark Slc34a2  TWKFLPIWLRSLEPWDRVMQRFTD----IFCCCC-------K-------KKC----------SNKMNKKEKGIKS----FE
Lizard Slc34a2          NWGFLPKWMRSLEPWDNVVTSVSS-TCGRCCCCC-------C-------KCCR--RD------KGEDVAKEKPTKS----LE
Chicken Slc34a2         NWDFLPIWMHSLEPWDNMIMSSLA-FCGKHCCGF-------C-------KCCKVN--------AEQEGAKDNQLKT----ME
Cow Slc34a3             SWAWLPLWLRSLEPWDLLVRR---------CCPC---------------KACSPPQAVAKE-----------------TH
Opossum Slc34a3         SWAFLPLWLHSLQPWDRAITG---------CCRC---------------CPRAHH-------EDSAGAALKE-------AQ
Elephant Slc34a3        SWAWLPHWLHSLEPWDGLVTH---------CCPC---------------QACSAPHATTKK-----------------AH
Human Slc34a3           SWAWLPVWLHSLEPWDRLVTR---------CCPC---------------NVCSPPKATTKE-----------------AY
Mouse Slc34a3           SWAWLPLWLHSLEPWDRLVTA---------CCPC---------------RACSNSPMTSKV-----------------AH
Rat Slc34a3             SWAWLPLWLHSLEPWDRLVTG---------CCPF---------------KAYSNSHMTSKV-----------------AH
Coelacanth Slc34a3      TWNFLPMWMHSLKPWDRLFSA---------CCT----------------NCFKCCKKQEGKGNSTAAAATELETAFGYNEPH
Frog Slc34a3            DWGFLPTWMHSLAPLDRLFSSVCG------CCC----------------KKCNKS--------EEEKPKEQLPADLSLGDMH
```

Fig. 9. Alignment of vertebrate Slc34a protein sequences showing characteristic motif conserved across members of the Slc34a2 group. The alignment shows the region around the portion identified as unique to rat Slc34a2 in comparison to rat Slc34a1 or Slc34a3 (see Fig. 1*C*). Highlighted in yellow are the homologous regions in other vertebrate Slc34a2 proteins, and in the Slc34a-type lamprey sequence. The characteristic Slc34a2 motif identified within this region contains at least three positive residues uninterrupted by any negatively charged residues, with the positive residues regularly spaced apart by at least four small residues (primarily cysteines). A Slc34a sequence containing this motif was found in all vertebrate species investigated. The only members of the Slc34a2 clade (see Fig. 8) where this motif was incomplete was are in the zebrafish and stickleback SLC34a2b (highlighted in blue). Positively charged residues are shown in bold and small amino acids are in italics. Sequence names correspond to the species and gene identifiers given in Supplemental Table S1 and to the phylogeny shown in Fig. 8. The incomplete spiny shark and skate NaPi-IIb sequences are omitted due to this region being missing from the EMBL/GenBank data. The alignment was generated using MUSCLE (http://www.ebi.ac.uk/Tools/msa/muscle/).

genes were observed in several fully sequenced genomes (e.g., zebrafish, chicken). This would suggest that the Slc34a2-group genes have a unique or important role whose loss cannot be complemented for by other transporters, and that this function is conserved across the jawed vertebrates. Common to all members of the Slc34a2 group, and to the homologous Slc34a2 gene in the lamprey, is a motif containing three positive amino acid residues (R, H, or K) separated by smaller uncharged residues (commonly C or S) (Fig. 9). This motif aligns with the unique predicted transmembrane domain noted above in the rat Slc34a2 gene (Fig. 1*C* and Table 2), and points towards an important functional role. Conserved positively charged amino acids have been noted in other Si-related proteins, such as the GRQ motifs of the SIT active Si transporters (32, 51). It may be postulated that these residues interact with local negative charges on the silicic acid molecule as part of a general biochemical basis for transmembrane Si transport.

Conclusions

The identification that Slc34a2 can transport Si in mammals establishes another distinct gene family of Si transporters that could be involved in the regulation of Si homeostasis and that bears no sequence similarity with known Si-related genes in plants, sponges, choanoflagellates, or diatoms, although it shows strong structural similarities to silicon exporters in plants. Crucially, our work is also one of the first pieces of evidence for a functionally relevant Si-responsive gene in mammals. In parallel with this work, Garneau et al. (18) and Deshmukh et al. (8) have recently identified Si-permeable aquaporins that appear to play an important role in Si influx. Coupled with the active efflux transporter that is reported herein, we propose a Si transport model in mammals that mirrors that known in plants (28), i.e., a model in which an influx and efflux transporter must be present to allow Si movement through cells. Here, Slc34a2 is effluxing H_4SiO_4 from the renal tubular epithelial cell into the circulation, i.e., it is involved in the reabsorption of H_4SiO_4 in the kidneys. As an inevitable consequence of this expression at this cellular location, phosphate will be moved in the opposing direction. Dietary Si-P interactions have been noted, with animals on a Si-deficient diet showing conserved bone Si levels but depleted bone P levels (24). Assuming Slc34a2 is similarly involved in bone conservation of Si as it is in the kidney then our results explain these observation (24). Finally, it is also interesting to note that Lsi2's are equally upregulated in plants in conditions of Si deprivation (34), a phenomenon that was instrumental in identifying Slc34a2 in this work. Collectively, our data provide indication that, rather than being a biochemically inert element, Si in fact plays a role in vertebrate physiology deserving of its preservation under exposure conditions of deprivation.

ACKNOWLEDGMENTS

We thank Dr. Paul Curnow (University of Bristol, UK) and Dr. Joanne Marks and Professor Robert Unwin (University College London, UK) for discussions and comments on the manuscript. The *Xenopus laevis* oocyte entry vector pT7TS (used for the Si transport studies) was a kind gift from Dr. Tony Miller (John Innes Centre, Norwich Research Park, Norwich, UK).

Present addresses: S. Ratcliffe, University of Bristol, School of Biochemistry, Medical Sciences Building, University Walk, Bristol BS8 1TD, UK; A. Marron, University of Cambridge, Department of Applied Maths and Theorectical Physics, Centre for Mathematical Sciences, Wilberforce Road, Cambridge CB3 0WA, UK; M. Müller, University of East Anglia, Norwich Medical School, Faculty of Medicine and Health Sciences, Norwich NR4 7TJ, UK.

GRANTS

This work was supported by Medical Research Council Grant MC_US_A090_0008/Unit Programme number U1059) (to J. J. Powell); Charitable Foundation of the Institute of Brewing and Distilling, UK (to S. Ratcliffe and R. Jugdaohsingh); Grant-in-Aid for Scientific Research on Innovative Areas from the Ministry of Education, Culture, Sports, Science and Technology of Japan (No. 22119002) (to J. F. Ma and N. Mitani-Ueno); Biotechnology and Biological Sciences Research Council (BBSRC) Comparative Genomics Training Grant BB/E527604/1 and a Leathersellers' Company Scholarship awarded by Fitzwilliam College, Cambridge (to A. Marron); Natural Sciences and Engineering Research Council of Canada (No. 364175) and Canada Foundation for Innovation (No. 950-205342) (to J. Vivancos, R. Deshmukh, and R. R. Bélanger); Netherlands Nutrigenomics Centre (to M. V. Boekschoten and M. Müller); Natural Sciences and Engineering Research Council of Canada (to S. D. Kinrade); and Canadian Institutes of Health Research (to P. Isenring).

DISCLOSURES

No conflicts of interest, financial or otherwise, are declared by the author(s).

AUTHOR CONTRIBUTIONS

S.R., R.J., J.V., A.M., R.D., N.M.-U., J.R., and M.V.B. performed experiments; S.R., R.J., J.V., A.M., J.F.M., N.M.-U., J.R., J.W., and M.V.B. analyzed data; S.R., R.J., R.D., J.R., J.W., R.C.M., S.D.K., P.I., R.R.B., and J.P. interpreted results of experiments; S.R., R.J., A.M., R.D., J.R., J.W., and R.C.M. prepared figures; S.R., R.J., and J.P. drafted manuscript; S.R., R.J., J.V., A.M., R.D., J.F.M., N.M.-U., M.V.B., R.C.M., S.D.K., P.I., R.R.B., and J.P. edited and revised manuscript; S.R., R.J., J.V., A.M., R.D., J.F.M., N.M.-U., M.V.B., M.M., R.C.M., S.D.K., P.I., R.R.B., and J.P. approved final version of manuscript.

REFERENCES

1. **Abascal F, Zardoya R, Posada D.** ProtTest: selection of best-fit models of protein evolution. *Bioinformatics* 21: 2104–2105, 2005. doi:10.1093/bioinformatics/bti263.
2. **Adamo C, Barone V.** Toward reliable density functional methods without adjustable parameters: the PBE0 model. *J Chem Phys* 110: 6158–6170, 1999. doi:10.1063/1.478522.
3. **Altschul SF, Madden TL, Schäffer AA, Zhang J, Zhang Z, Miller W, Lipman DJ.** Gapped BLAST and PSI-BLAST: a new generation of protein database search programs. *Nucleic Acids Res* 25: 3389–3402, 1997. doi:10.1093/nar/25.17.3389.
4. **Binning RC Jr, Curtiss LA.** Compact contracted basis-sets f or 3rd-row atoms - GA-KR. *J Comput Chem* 11: 1206–1216, 1990. doi:10.1002/jcc.540111013.
5. **Brzezinski MA, Olson RJ, Chisholm SW.** Silicon availability and cell-cycle progression in marine diatoms. *Mar Ecol Prog Ser* 67: 83–96, 1990. doi:10.3354/meps067083.
6. **Carlisle EM.** Silicon: an essential element for the chick. *Science* 178: 619–621, 1972. doi:10.1126/science.178.4061.619.
7. **Cossi M, Rega N, Scalmani G, Barone V.** Energies, structures, and electronic properties of molecules in solution with the C-PCM solvation model. *J Comput Chem* 24: 669–681, 2003. doi:10.1002/jcc.10189.
8. **Deshmukh RK, Vivancos J, Ramakrishnan G, Guérin V, Carpentier G, Sonah H, Labbé C, Isenring P, Belzile FJ, Bélanger RR.** A precise spacing between the NPA domains of aquaporins is essential for silicon permeability in plants. *Plant J* 83: 489–500, 2015. doi:10.1111/tpj.12904.
9. **Ditchfield R, Hehre WJ, Pople JA.** Self-consistent molecular orbital methods. 9. Extended gaussian-type basis for molecular-orbital studies of organic molecules. *J Chem Phys* 54: 724–728, 1971. doi:10.1063/1.1674902.
10. **Duncan AE, Munn-Chernoff MA, Hudson DL, Eschenbacher MA, Agrawal A, Grant JD, Nelson EC, Waldron M, Glowinski AL, Sartor CE, Bucholz KK, Madden PAF, Heath AC.** Genetic and environmental risk for major depression in African-American and European-American women. *Twin Res Hum Genet* 17: 244–253, 2014. doi:10.1017/thg.2014.28.

11. **Durak GM, Taylor AR, Walker CE, Probert I, de Vargas C, Audic S, Schroeder D, Brownlee C, Wheeler GL.** A role for diatom-like silicon transporters in calcifying coccolithophores. *Nat Commun* 7: 10543, 2016. doi:10.1038/ncomms10543.
12. **Epstein E.** The anomaly of silicon in plant biology. *Proc Natl Acad Sci USA* 91: 11–17, 1994. doi:10.1073/pnas.91.1.11.
13. **Fauteux F, Chain F, Belzile F, Menzies JG, Bélanger RR.** The protective role of silicon in the Arabidopsis-powdery mildew pathosystem. *Proc Natl Acad Sci USA* 103: 17554–17559, 2006. doi:10.1073/pnas.0606330103.
14. **Forster IC, Hernando N, Biber J, Murer H.** Proximal tubular handling of phosphate: A molecular perspective. *Kidney Int* 70: 1548–1559, 2006. doi:10.1038/sj.ki.5001813.
15. **Francl MM, Pietro WJ, Hehre WJ, Binkley S, Gordon MS, DeFrees DJ, Pople JA.** Self-consistent molecular orbital methods. XXIII. A polarization-type basis set for second-row elements. *J Chem Phys* 77: 3654–3665, 1982. doi:10.1063/1.444267.
16. **Frisch MJ, Pople JA, Binkley JS.** Self-consistent molecular orbital methods. 25. Supplementary functions for gaussian basis sets. *J Chem Phys* 80: 3265–3269, 1984. doi:10.1063/1.447079.
17. **Frisch MJ, Trucks GW, Schlegel HB, Scuseria GE, Robb MA, Cheeseman JR, Scalmani G, Barone V, Mennucci B, Petersson GA, Nakatsuji H, Caricato M, Li X, Hratchian HP, Izmaylov AF, Bloino J, Zheng G, Sonnenberg JL, Hada M, Ehara M, Toyota K, Fukuda R, Hasegawa J, Ishida M, Nakajima T, Honda Y, Kitao O, Nakai H, Vreven T, Montgomery Jr JA, Peralta JE, Ogliaro F, Bearpark M, Heyd JJ, Brothers E, Kudin KN, Staroverov VN, Kobayashi R, Normand J, Raghavachari K, Rendell A, Burant JC, Iyengar SS, Tomasi J, Cossi M, Rega N, Millam JM, Klene M, Knox JE, Cross JB, Bakken V, Adamo C, Jaramillo J, Gomperts R, Stratmann RE, Yazyev O, Austin AJ, Cammi R, Pomelli C, Ochterski JW, Martin RL, Morokuma K, Zakrzewski VG, Voth GA, Salvador P, Dannenberg JJ, Dapprich S, Daniels AD, Farkas Ö, Foresman JB, Vincent Ortiz JV, Cioslowski J, Fox DJ.** Gaussian09, Revision D.01. Wallingford, CT: Gaussian, 2009. Available at http://gaussian.com/glossary/g09/.
18. **Garneau AP, Carpentier GA, Marcoux AA, Frenette-Cotton R, Simard CF, Rémus-Borel W, Caron L, Jacob-Wagner M, Noël M, Powell JJ, Bélanger R, Côté F, Isenring P.** Aquaporins mediate silicon transport in humans. *PLoS One* 10: e0136149, 2015. doi:10.1371/journal.pone.0136149.
19. **Guindon S, Dufayard JF, Lefort V, Anisimova M, Hordijk W, Gascuel O.** New algorithms and methods to estimate maximum-likelihood phylogenies: assessing the performance of PhyML 3.0. *Syst Biol* 59: 307–321, 2010. doi:10.1093/sysbio/syq010.
20. **Hehre WJ, Ditchfield R, Pople JA.** Self-consistent molecular orbital methods. 12. Further extensions of gaussian-type basis sets for use in molecular-orbital studies of organic-molecules. *J Chem Phys* 56: 2257–2261, 1972. doi:10.1063/1.1677527.
21. **Hildebrand M, Higgins DR, Busser K, Volcani BE.** Silicon-responsive cDNA clones isolated from the marine diatom *Cylindrotheca fusiformis*. *Gene* 132: 213–218, 1993. doi:10.1016/0378-1119(93)90198-C.
22. **Hildebrand M, Volcani BE, Gassmann W, Schroeder JI.** A gene family of silicon transporters. *Nature* 385: 688–689, 1997. doi:10.1038/385688b0.
23. **Hilfiker H, Hattenhauer O, Traebert M, Forster I, Murer H, Biber J.** Characterization of a murine type II sodium-phosphate cotransporter expressed in mammalian small intestine. *Proc Natl Acad Sci USA* 95: 14564–14569, 1998. doi:10.1073/pnas.95.24.14564.
24. **Jugdaohsingh R, Calomme MR, Robinson K, Nielsen F, Anderson SHC, D'Haese P, Geusens P, Loveridge N, Thompson RPH, Powell JJ.** Increased longitudinal growth in rats on a silicon-depleted diet. *Bone* 43: 596–606, 2008. doi:10.1016/j.bone.2008.04.014.
25. **Jugdaohsingh R, Tucker KL, Qiao N, Cupples LA, Kiel DP, Powell JJ.** Dietary silicon intake is positively associated with bone mineral density in men and premenopausal women of the Framingham Offspring cohort. *J Bone Miner Res* 19: 297–307, 2004. doi:10.1359/JBMR.0301225.
26. **Lartillot N, Philippe H.** A Bayesian mixture model for across-site heterogeneities in the amino-acid replacement process. *Mol Biol Evol* 21: 1095–1109, 2004. doi:10.1093/molbev/msh112.
27. **Ma JF, Tamai K, Ichii M, Wu GF.** A rice mutant defective in Si uptake. *Plant Physiol* 130: 2111–2117, 2002. doi:10.1104/pp.010348.
28. **Ma JF, Yamaji N.** A cooperative system of silicon transport in plants. *Trends Plant Sci* 20: 435–442, 2015. doi:10.1016/j.tplants.2015.04.007.
29. **Ma JF, Tamai K, Yamaji N, Mitani N, Konishi S, Katsuhara M, Ishiguro M, Murata Y, Yano M.** A silicon transporter in rice. *Nature* 440: 688–691, 2006. doi:10.1038/nature04590.
30. **Ma JF, Yamaji N, Mitani N, Tamai K, Konishi S, Fujiwara T, Katsuhara M, Yano M.** An efflux transporter of silicon in rice. *Nature* 448: 209–212, 2007. doi:10.1038/nature05964.
31. **Marks J, Debnam ES, Unwin RJ.** Phosphate homeostasis and the renal-gastrointestinal axis. *Am J Physiol Renal Physiol* 299: F285–F296, 2010. doi:10.1152/ajprenal.00508.2009.
32. **Marron AO, Alston MJ, Heavens D, Akam M, Caccamo M, Holland PWH, Walker G.** A family of diatom-like silicon transporters in the siliceous loricate choanoflagellates. *Proc Biol Sci* 280: 20122543, 2013. doi:10.1098/rspb.2012.2543.
33. **Meyer A, Zardoya R.** Recent advances in the (molecular) phylogeny of vertebrates. *Annu Rev Ecol Evol Syst* 34: 311–338, 2003. doi:10.1146/annurev.ecolsys.34.011802.132351.
34. **Mitani N, Chiba Y, Yamaji N, Ma JF.** Identification and characterization of maize and barley Lsi2-like silicon efflux transporters reveals a distinct silicon uptake system from that in rice. *Plant Cell* 21: 2133–2142, 2009. doi:10.1105/tpc.109.067884.
35. **Mitani N, Yamaji N, Ma JF.** Characterization of substrate specificity of a rice silicon transporter, Lsi1. *Pflugers Arch* 456: 679–686, 2008. doi:10.1007/s00424-007-0408-y.
36. **Murer H, Forster I, Biber J.** The sodium phosphate cotransporter family SLC34. *Pflugers Arch* 447: 763–767, 2004. doi:10.1007/s00424-003-1072-5.
37. **Onsager L.** Electric moments of molecules in liquids. *J Am Chem Soc* 58: 1486–1493, 1936. doi:10.1021/ja01299a050.
38. **Perdew JP, Burke K, Ernzerhof M.** Errata: generalized gradient approximation made simple. *Phys Rev Lett* 78: 1396, 1997. doi:10.1103/PhysRevLett.78.1396.
39. **Perdew JP, Burke K, Ernzerhof M.** Generalized gradient approximation made simple. *Phys Rev Lett* 77: 3865–3868, 1996. doi:10.1103/PhysRevLett.77.3865.
40. **Preston GM, Carroll TP, Guggino WB, Agre P.** Appearance of water channels in *Xenopus* oocytes expressing red cell CHIP28 protein. *Science* 256: 385–387, 1992. doi:10.1126/science.256.5055.385.
41. **Rassolov VA, Pople JA, Ratner MA, Windus TL.** 6-31G* basis set for atoms K through Zn. *J Chem Phys* 109: 1223–1229, 1998. doi:10.1063/1.476673.
42. **Rassolov VA, Ratner MA, Pople JA, Redfern PC, Curtiss LA.** 6-31G* basis set for third-row atoms. *J Comput Chem* 22: 976–984, 2001. doi:10.1002/jcc.1058.
43. **Reffitt DM, Ogston N, Jugdaohsingh R, Cheung HFJ, Evans BAJ, Thompson RPH, Powell JJ, Hampson GN.** Orthosilicic acid stimulates collagen type 1 synthesis and osteoblastic differentiation in human osteoblast-like cells in vitro. *Bone* 32: 127–135, 2003. doi:10.1016/S8756-3282(02)00950-X.
44. **Sartor MA, Tomlinson CR, Wesselkamper SC, Sivaganesan S, Leikauf GD, Medvedovic M.** Intensity-based hierarchical Bayes method improves testing for differentially expressed genes in microarray experiments. *BMC Bioinformatics* 7: 538, 2006. doi:10.1186/1471-2105-7-538.
45. **Schwarz K, Milne DB.** Growth-promoting effects of silicon in rats. *Nature* 239: 333–334, 1972. doi:10.1038/239333a0.
46. **Sha Q, Pearson W, Burcea LC, Wigfall DA, Schlesinger PH, Nichols CG, Mercer RW.** Human FXYD2 G41R mutation responsible for renal hypomagnesemia behaves as an inward-rectifying cation channel. *Am J Physiol Renal Physiol* 295: F91–F99, 2008. doi:10.1152/ajprenal.00519.2007.
47. **Shilton BH.** Active transporters as enzymes: an energetic framework applied to major facilitator superfamily and ABC importer systems. *Biochem J* 467: 193–199, 2015. doi:10.1042/BJ20140675.
48. **Stamm M, Staritzbichler R, Khafizov K, Forrest LR.** Alignment of helical membrane protein sequences using AlignMe. *PLoS One* 8: e57731, 2013. doi:10.1371/journal.pone.0057731.
49. **Storey JD, Tibshirani R.** Statistical significance for genomewide studies. *Proc Natl Acad Sci USA* 100: 9440–9445, 2003. doi:10.1073/pnas.1530509100.
50. **Suyama T, Okada S, Ishijima T, Iida K, Abe K, Nakai Y.** High phosphorus diet-induced changes in NaPi-IIb phosphate transporter expression in the rat kidney: DNA microarray analysis. *PLoS One* 7: e29483, 2012. doi:10.1371/journal.pone.0029483.
51. **Thamatrakoln K, Alverson AJ, Hildebrand M.** Comparative sequence analysis of diatom silicon transporters: toward a mechanistic model of

silicon transport. *J Phycol* 42: 822–834, 2006. doi:10.1111/j.1529-8817.2006.00233.x.

52. **Tomasi J, Mennucci B, Cancès E.** The IEF version of the PCM solvation method: an overview of a new method addressed to study molecular solutes at the QM ab initio level. *J Mol Struct* 464: 211–226, 1999. doi:10.1016/S0166-1280(98)00553-3.
53. **Viklund H, Elofsson A.** OCTOPUS: improving topology prediction by two-track ANN-based preference scores and an extended topological grammar. *Bioinformatics* 24: 1662–1668, 2008. doi:10.1093/bioinformatics/btn221.
54. **Villa-Bellosta R, Sorribas V.** Role of rat sodium/phosphate cotransporters in the cell membrane transport of arsenate. *Toxicol Appl Pharmacol* 232: 125–134, 2008. doi:10.1016/j.taap.2008.05.026.
55. **Wagner CA, Hernando N, Forster IC, Biber J.** The SLC34 family of sodium-dependent phosphate transporters. *Pflugers Arch* 466: 139–153, 2014. doi:10.1007/s00424-013-1418-6.
56. **Wong MW, Frisch MJ, Wiberg KB.** Solvent effects 1. The mediation of electrostatic effects by solvents. *J Am Chem Soc* 113: 4776–4782, 1991. doi:10.1021/ja00013a010.
57. **Wong MW, Wiberg KB, Frisch MJ.** Hartree-Fock second derivatives and electric field properties in a solvent reaction field - theory and application. *J Chem Phys* 95: 8991–8998, 1991. doi:10.1063/1.461230.
58. **Wu Z, Irizarry RA, Gentleman R, Martinez-Murillo F, Spencer F.** A model based background adjustment for oligonucleotide expression arrays. *J Am Stat Assoc* 99: 909–917, 2004. doi:10.1198/016214504000000683.